ARTICLES

Measurement of $\vec{\gamma}d \rightarrow pn\pi^0$ at large nucleon momenta

G. S. Adams,[2] H. Baghaei,[5] A. Caracappa,[1] W. Clayton,[2] A. D'Angelo,[3] S. Hoblit,[5] M. Khandaker,[6] O. C. Kistner,[1] T. Kobayashi,[2] R. Lindgren,[5] L. Miceli,[1] C. Ruth,[2] A. M. Sandorfi,[1] C. Schaerf,[3] R. M. Sealock,[5] L. C. Smith,[5] P. Stoler,[5] D. J. Tedeschi,[2] C. E. Thorn,[1] S. T. Thornton,[5] K. Vaziri,[2,*] C. S. Whisnant,[4] and E. J. Winhold[2]

[1]*Physics Department, Brookhaven National Laboratory, Upton, New York 11973*

[2]*Physics Department, Rensselaer Polytechnic Institute, Troy, New York 12180*

[3]*Instituto Nazionale di Fisice Nucleare, Sezione di Roma 2, and Università di Roma Tor Vergata, Via della Ricerca Scientifica 1, I00133-Rome, Italy*

[4]*Physics Department, University of South Carolina, Columbia, South Carolina 29208*

[5]*Physics Department, University of Virginia, Charlottesville, Virginia 22903*

[6]*Physics Department, Virginia Polytechnic Institute and State University, Blacksburg, Virginia 24061*

(Received 1 August 1994)

Coincident protons and neutrons from the reaction $\vec{\gamma}d \rightarrow pn\pi^0$ were measured at a photon energy of 290 MeV. Cross sections and beam asymmetries were extracted for nucleon momenta above the quasifree region for the first time. The measured cross sections are compared with the results of a cascade Monte Carlo calculation.

PACS number(s): 25.20.Lj, 24.70.+s, 14.20.Gk

I. INTRODUCTION

The N-$\Delta(1232)$ system occupies a unique position as the lightest two-baryon state above the two-nucleon mass. However little is known about N-Δ scattering. Precise knowledge of the N-Δ interaction is needed for a consistent treatment of the πNN system, as well as the off-shell behavior of the NN potential [1].

The N-Δ interaction is best studied in few-body reactions since there the wave functions are more easily calculated and medium modifications from propagation in the nuclear environment are reduced. Several recent theoretical analyses have investigated the effects of N-Δ coupled channels in pion and proton induced reactions [2–4]. Those works yield inconclusive results, since including the N-Δ terms often results in poor agreement with experiment. Theoretical predictions including N-Δ scattering exist for the photon-induced reactions $\gamma d \rightarrow pn$ and $\gamma d \rightarrow \pi^0 d$ as well [4]. Also, Laget predicts substantial effects on the cross section for $\gamma d \rightarrow pp\pi^-$ when N-Δ scattering is included in the intermediate state [5]. However, the published data for that reaction are insufficient to make a detailed comparison with theory [6]. Theoretical analyses of the hadronic reactions have benefitted from the existence of plentiful polarization data but the same cannot be said for photoproduction. We expect that polarized photon experiments will help to distinguish the effects of N-Δ scattering from final-state NN and πN interactions.

The purpose of the present experiment was to provide data which can be used to further test the coupled channel models of few body systems, specifically in the πNN final state. The reaction $\vec{\gamma}d \rightarrow pn\pi^0$ was chosen because the elementary amplitude for π^0 production on the nucleon is dominated by the $\Delta(1232)$ resonance. Therefore the relative contribution from Δ-N scattering in the intermediate state should be enhanced in the present case over that for charged-pion photoproduction. The measurements were performed with polarized photons in the energy range E_γ = 190–300 MeV. The present paper reports most of the data from 274 to 304 MeV (average energy =290 MeV). These data are compared with the results of a cascade Monte Carlo calculation which includes the effects of πN and NN final state interactions. Substantial disagreement is observed between the cascade results and some of the data, indicating that reaction mechanisms other than quasifree absorption may be needed.

II. EXPERIMENT

The measurements were performed at the Laser Electron Gamma Source at Brookhaven National Laboratory. The beam was prepared by scattering polarized laser light from 2.5 GeV electrons. This produced a linearly polarized gamma beam with 99% polarization at 290 MeV. Beam polarization was calculated using the measured value of the laser polarization and the kinematics of Klein-Nishina scattering. Photon energies were tagged by measuring the scattered electron energies in

*Present address: Fermilab, MS 119 ES&H, Box 500, Batavia, IL 60510.

a magnetic spectrometer [7]. Multiple tagger hits were rejected in the analysis, giving an average tagging efficiency of about 75 percent. The resulting resolution in photon energy was about 5.5 MeV FWHM. The average beam rate for the experiment was typically 3×10^6 photons per second integrated over the full tagger range. Integrated beam intensity was measured with three e^+e^- pair-production monitors located downstream of the target. These were periodically calibrated to a sodium iodide scintillator at low beam rates.

The beam impinged on a liquid deuterium target operated at a temperature of 23 K and pressure equal to 20 psi (absolute). The beam profile on target was approximately elliptical with major and minor axes of 4.2 and 2.7 cm, respectively. A cylindrical target cell with spherical end caps was used. It was made of Ni, electroformed to a thickness of 0.012 cm, with a diameter of 5.0 cm. The maximum deuterium thickness presented to the beam was 10 cm (1.574 ± 0.005 g/cm^3). In the final data analysis contributions from the target cell walls were accounted for by subtracting data taken with the target cell empty. In all cases these background yields were less than 20 percent of the total yield.

Coincident protons and neutrons were detected in two scintillator arrays located on opposite sides of the beam. Protons were detected in CaF_2/plastic scintillator telescopes which were placed at 20° intervals (see Fig. 1). The forward-angle detectors located at laboratory scattering angles of 20° and 40° yielded the highest event rates. Those data are discussed in this paper. Protons were identified by their correlated dE, E signature. Energy calibration came from measurements of deuteron photodisintegration made before and after the photoproduction measurements. The proton energy resolution was typically 6% FWHM. Trigger thresholds for the 20° and 40° detectors were at kinetic energies equal to 48 and 42 MeV, respectively. These high detection thresholds were designed to give low detection efficiencies for spectator protons accompanying quasifree pion production from the neutron in deuterium.

An array of plastic scintillator telescopes was arranged in the same geometry as previous photodistintegration experiments to detect neutrons [8]. These telescopes consisted of a veto paddle (to distinguish charged particles) and two bar-shaped scintillators, each 10 cm thick and 160 cm long, stacked one behind the other. Each telescope subtended a solid angle of 0.11 sr. Each bar was viewed with photomultipliers at both ends. The light propagation time to each photomultiplier was used to locate the conversion point of the neutron. The data were binned according to the central angle of the neutron telescopes, θ_n, measured in the gamma-proton plane. These telescopes were centered every 8° with $20° \leq \theta_n \leq 140°$. Neutrons were identified by requiring no charged particles in any veto paddle, and cutting on the time of flight (TOF) to reject photons. The average flight path from target to detector was 110 cm. This TOF information was then used to construct velocity and neutron momentum, yielding an overall momentum resolution $dP/P \approx 0.10$ FWHM. The conversion efficiency of each detector was calculated with the Kent State Monte Carlo code [9]. The accuracy of the calculated efficiency is expected to be about ±5%, based on previous photodisintegration measurements with the same apparatus [8].

A cut on the missing mass of pn pairs was used to identify events from the reaction $\vec{\gamma}d \rightarrow pn\pi^0$. Events that fell outside the π^0 window were rejected as being due to deuteron photodisintegration, background, or reactions in the scintillators. The kinematics of the final events was overdetermined by one variable, allowing a

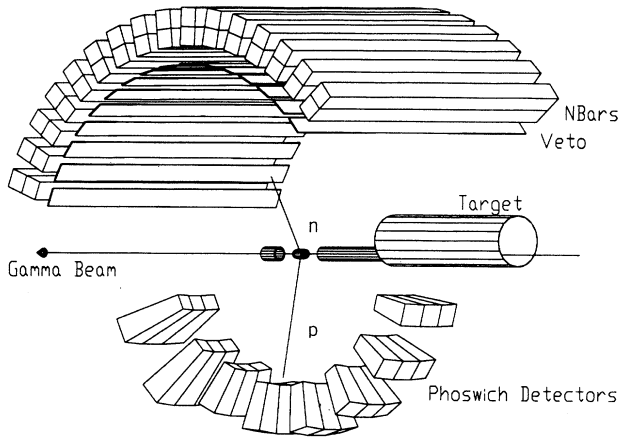

FIG. 1. Experimental apparatus. The lower scintillator array detected protons and the upper array detected neutrons.

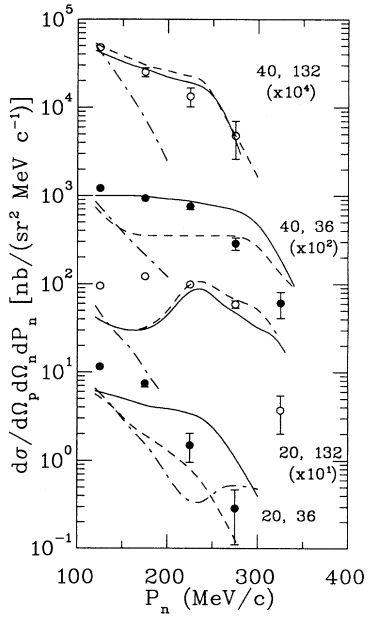

FIG. 2. Cross section as a function of neutron momentum, at correlated angles θ_p, θ_n. All proton momenta above detection threshold are summed in the figure. The cascade model predictions are shown for the spectator model (dot-dashed curve), spectator plus πN final state interactions (dashed curve), and spectator plus πN and NN final state interactions (solid curve).

consistency check between the photon energy measured with the tagger and that calculated from the pn measurements. An additional one percent of events was rejected as having a calculated energy which did not correlate with the measured value.

The final data are plotted in Figs. 2, 3, and 4, and listed in Tables I and II. Only statistical error bars are shown in the figures. An additional systematic error of 8.2 percent was assigned to the absolute cross section by adding in quadrature the components listed in Table III. Figure 2 shows the measured neutron-momentum spectra at four correlated pn angle pairs. The data from four adjacent neutron telescopes are summed in the figure ($\Delta\theta_n \pm 16°$). The data are also summed over the full proton momentum range above the detection threshold and over the full azimuthal acceptance of each bar, which is a function of θ_n (see Fig. 5). These data can be compared with the spectator-momentum distributions which have been measured for quasi-free π-production from deuterium [10]. In that case a quasifree peak is evident at a momentum of 60 MeV/c and the distribution falls monotonically up to momenta in excess of 200 MeV/c. Some of the data in Fig. 2 have distributions which differ markedly from this quasifree picture. The data at $\theta_p = 20°$, $\theta_n = 132°$ are particularly noteworthy since they exhibit a broad peak at 175 MeV/c.

Figures 3 and 4 show the angular distributions of the cross section and beam asymmetry for $\theta_p = 20°$ and 40° respectively. These data are integrated over the proton momentum range over threshold, and over the neutron momentum range $100 \leq p_n \leq 200$ MeV/c. It is reasonable to compare the present asymmetry data with the values expected for quasifree pion production. The appropriate comparison is for the reaction $\vec{\gamma}p \to p\pi^0$. The VPI multipole analysis for this channel yields values of -0.42 at $\theta_p = 20°$ and -0.50 at $\theta_p = 40°$ [11,12]. Comparison with Figs. 3 and 4 reveals that the present data do not resemble what one would expect from quasifree π^0 production. The measured asymmetries are negative, but not constant, at $\theta_p = 40°$, and the data are close to zero at $\theta_p = 20°$. This observation is perhaps not very surprising since final-state interactions (FSI) should play an important role in determining the neutron angular distributions for momenta above the quasifree peak.

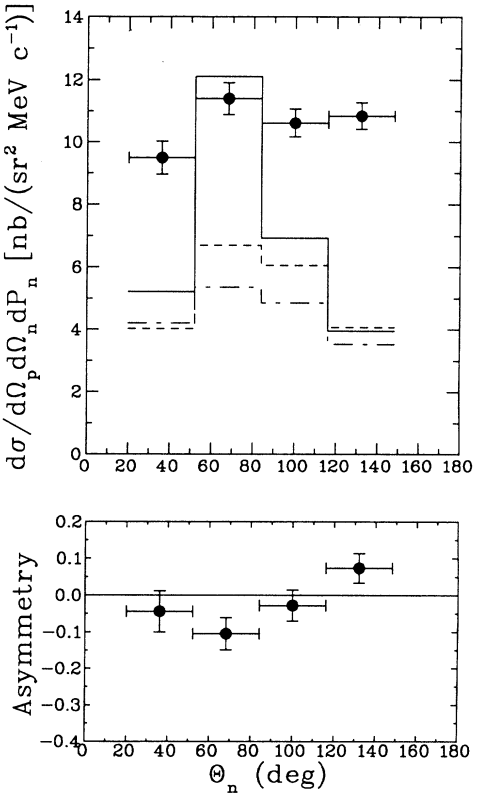

FIG. 3. Cross section and beam symmetry $(\sigma_\parallel - \sigma_\perp / \sigma_\parallel + \sigma_\perp)$ as a function of neutron central angle, at $\theta_p = 20°$ and $p_n = 100$–200 MeV/c. All proton momenta above detection threshold are summed in the figure. The cascade model predictions are shown for the spectator model (dot-dashed curve), spectator plus πN final state interactions (dashed curve), and spectator plus πN and NN final state interactions (solid curve).

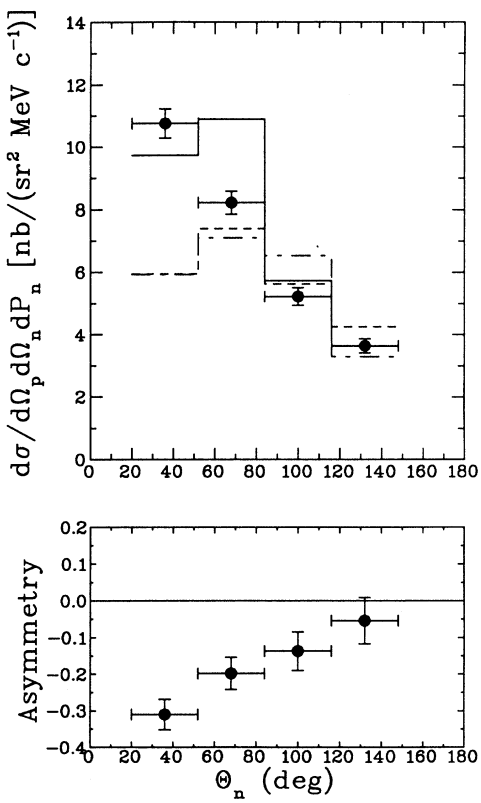

FIG. 4. Cross section and beam symmetry $(\sigma_\parallel - \sigma_\perp / \sigma_\parallel + \sigma_\perp)$ as a function of neutron central angle, at $\theta_p = 40°$ and $p_n = 100$–200 MeV/c. All proton momenta above detection threshold are summed in the figure. The cascade model predictions are shown for the spectator model (dot-dashed curve), spectator plus πN final state interactions (dashed curve), and spectator plus πN and NN final state interactions (solid curve).

TABLE I. Experimental neutron momentum distributions. Data are tabulated by detector central angles and summed over the momentum of the proton and the full angular acceptance of the detectors.

θ_p (deg)	θ_n (deg)	p_n (MeV/c)	σ $\left(\frac{\text{nb}}{\text{sr}^2}\frac{\text{MeV}}{\text{c}}\right)$	ε_σ $\left(\frac{\text{nb}}{\text{sr}^2}\frac{\text{MeV}}{\text{c}}\right)$
40	132	125	4.78	0.35
		175	2.51	0.30
		225	1.33	0.32
		275	0.48	0.22
40	36	125	12.20	0.70
		175	9.32	0.64
		225	7.58	0.67
		275	2.86	0.46
		325	0.61	0.20
20	132	125	9.52	0.54
		175	12.17	0.68
		225	9.90	0.75
		275	5.91	0.58
		325	0.37	0.17
20	36	125	11.52	0.79
		175	7.46	0.71
		225	1.49	0.53
		275	0.29	0.18

III. CASCADE MONTE CARLO

The authors are unaware of any published theoretical calculations for the $pn\pi^0$ final state which are pertinent to the present data. Therefore we have constructed a cascade Monte Carlo model in order to analyze the quasifree component of the data and to investigate the qualitative effects of NN and πN FSI. In this model the free cross sections for $\gamma p \to p\pi^0$ and $\gamma n \to n\pi^0$ were extracted from the SAID database [11] and used to generate quasifree Monte Carlo events in deuterium. The basis for this part of the calculation is the spectator model of Ref. [13]. Final state interactions of the np and $n\pi^0$ pairs were added by sampling the on-shell elastic differential cross sections, again taken from the SAID database [12]. In the case of $n\pi^0$ scattering an isospin decomposition of the charged πN channels was used to construct the cross section. Further details of the analysis can be found in Ref. [14].

The cascade method was tested by changing the event generator to produce π^- events and predicting the known quasifree cross sections for $\gamma d \to pp\pi^-$ as a function of pion momentum (see Fig. 20 in Ref. [15]). The present model produces agreement within the experimental error bars of the data. We have also tested the model against data [6] in the recoil-proton momentum range $130 \leq p_r \leq 170$ MeV/c. In that case the data show deviations from the quasifree model (no final state interactions) of up to 20% in the differential cross section. No absolute cross sections are available for comparison. The present cascade model accounts for the data at proton angles up to 120° quite well, but predicts deviations from the quasifree value which are 50 percent too small at 150°. From these comparisons we estimate that the cascade model accuracy predicts quasifree pion production including the effects of FSI to within at worst a factor of 2 in the differential cross section.

The momentum distributions predicted with the cascade method are compared with the present data in Fig. 2. From this comparison it is evident that FSI pro-

TABLE II. Angular distributions of the cross section and beam asymmetry $(\sigma_\parallel - \sigma_\perp/\sigma_\parallel + \sigma_\perp)$. Data have been summed over the angular acceptance of the detectors and over the neutron momentum range $p_n = 100$–200 MeV/c.

θ_p (deg)	θ_n (deg)	σ $\left(\frac{\text{nb}}{\text{sr}^2}\frac{\text{MeV}}{\text{c}}\right)$	ε_σ $\left(\frac{\text{nb}}{\text{sr}^2}\frac{\text{MeV}}{\text{c}}\right)$	Σ	ε_Σ
20	36	9.49	0.53	−0.440	0.056
	68	11.40	0.51	−0.105	0.044
	100	10.61	0.45	−0.028	0.042
	132	10.84	0.43	+0.074	0.040
40	36	10.76	0.47	−0.310	0.042
	68	8.22	0.37	−0.198	0.044
	100	5.23	0.28	−0.137	0.053
	132	3.64	0.23	−0.054	0.063

TABLE III. Contributions to the systematic error in the absolute cross section. These contributions are added in quadrature to produce the total uncertainty.

Source	σ (%)
Ω_p	3.1
Ω_n	1.0
p efficiency	3.0
n efficiency	5.0
π cut eff.	2.0
ρ_{target}	1.0
L_{target}	2.0
Beam flux	3.7
Total	8.2

duce rather modest effects at low momentum. At around 125 MeV/c the tail of the spectator-neutron peak (dot-dashed curve) is visible when coincident protons are detected at 40°. At 270 MeV/c the model predicts a small peak from quasifree π^0 production on the neutron (dot-dashed curve, shown only for $\theta_p = 20°$, $\theta_n = 36°$). This channel is suppressed relative to production on the proton because of the high proton energy threshold in the experiment. This peak goes away when FSI are included in the model. The effects of including FSI are most evident in the momentum range from 200 to 300 MeV/c. The dashed curve in Fig. 2 includes πN FSI and the full curve includes πN and NN FSI. As one can see from the figure, πN FSI are substantial at all angles and they generally improve the agreement with the data. The full calculation including πN and NN FSI usually lies within a factor of 2 of the measured cross sections, except at correlated angles $\theta_p = 20°$, $\theta_p = 132°$. For these data the model shows substantial contributions from πN rescattering, but rather small contributions from NN FSI. The πN scattered events form a broad peak at about 240 MeV/c which can be interpreted as the effect of finite angular acceptance. That is, quasifree pion production at a pion angle of 122° results in a recoiling proton at 20° and a pion energy of about 74 MeV. When the pion scatters from the neutron with a relative recoil-neutron angle of 10°, the resulting neutron emerges at a laboratory angle of 132° and momentum equal to 260 MeV/c. While the predicted strength in the region of this peak is in good agreement with the data, the model predicts a cross section at 160 MeV/c which is nearly a factor of 4 too small. At this momentum the cascade model predicts a minimum in the distribution but the data show a broad peak. The NN FSI do little to fill in this minimum because of the large angular separation between proton and neutron. In the cascade model the maximum angular separation between a quasifree proton, which always goes forward, and a neutron resulting from FSI is about 90°. This corresponds to small-angle scattering of the proton on the neutron. The data under discussion ($\theta_p = 20°$, $\theta_n = 132°$) have proton-neutron separation angles approximately equal to 152° in the laboratory. By contrast, NN FSI dominate at $\theta_n = 36°$ for both proton angles, where the opening angles are smaller. Since the predicted effects from FSI are small at 160 MeV/c it seems unlikely that the errors inherent in the Monte Carlo cascade model (lack of off-shell effects, for example) can account for the discrepancy between the cascade model and the 132° data.

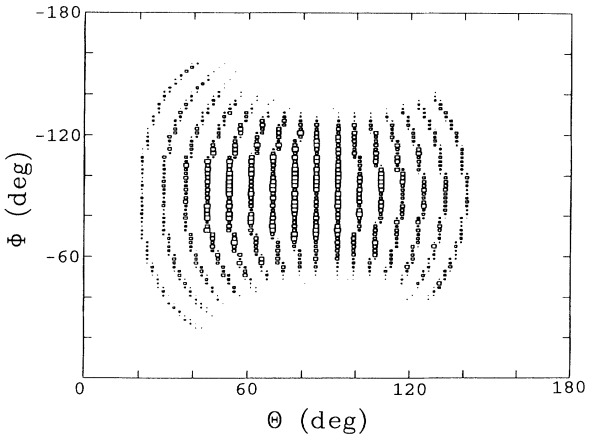

FIG. 5. Angular distribution of all neutrons, showing the angular acceptance of the neutron detectors in spherical polar coordinates. In these coordinates the neutron detectors are centered on $\phi = -90°$, and the proton detectors are centered on $\phi = +90°$.

This striking disagreement with the data is brought out more clearly in the angular distributions of the differential cross sections, for p_n = 100–200 MeV/c. At $\theta_p = 40°$ the cascade calculation is in fair agreement with the neutron angular distribution (Fig. 4). However the predicted angular distribution at $\theta_p = 20°$ (Fig. 3) is characterized by a sharp peak at about 70°, while the data are nearly constant at all angles. It is also noteworthy that the angular distribution of the beam asymmetry measured at $\theta_p = 20°$ differs markedly from the one measured at $\theta_p = 40°$. These observations suggest that new absorption mechanisms may be manifest in the data.

One mechanism that could be important is $n\Delta^+$ scattering in the intermediate state. Laget has investigated $p\Delta^0$ scattering in the reaction $\gamma d \rightarrow pp\pi^-$ at $E_\gamma = 317$ MeV. He finds that the theoretical cross sections increase up to 60 percent at recoil momentum $p_p = 160$ MeV/c when this intermediate rescattering channel is included [5]. It is noteworthy that we observe large deviations from the cascade model predictions at the same spectator momentum. In Laget's multiple scattering theory this momentum emerges in a natural way; when the initial proton and neutron are moving each with momentum 160 MeV/c and a real $\Delta(1232)$ resonance is produced in a head-on collision between the beam photon and one nucleon, the resulting $N\Delta$ pair has a low relative velocity. Under these conditions the S-wave interaction of the $N\Delta$ pair is enhanced and the scattered nucleon emerges with its laboratory momentum nearly unchanged. Unfortunately the paucity of data for π^- production does not allow a meaningful test of the theory [5]. It is hoped that the present data on π^0 production will stimulate further theoretical work in this area.

IV. SUMMARY AND CONCLUSIONS

We have measured cross sections and beam asymmetries for the reaction $\vec{\gamma}d \to pn\pi^0$. Quasifree production mechanisms are suppressed in the data due to the high momentum thresholds for proton and neutron detection. The bulk of the data are consistent with the predictions of a cascade Monte Carlo calculation which includes the effects of πN and NN final state interactions. However the predicted cross sections at $\theta_p = 20°$ and neutron momentum between 100 and 200 MeV/c are in marked contrast to the data. These results suggest that theoretical work in this area should be extended to include π^0 production with polarized photons.

ACKNOWLEDGMENTS

This work was supported in part by U.S. Department of Energy under Contract No. DE-AC02-76-CH00016, the National Science Foundation, and the Instituto Nazionale di Fisica Nucleare.

[1] W. A. Schnizer and W. Plessas, Phys. Rev. C **41**, 1095 (1990).
[2] C. Alexandrou and B. Blankleider, Phys. Rev. C **42**, 517 (1990).
[3] Erasmo Ferreira, Sarah C. B. Andrade, and H. G. Dosch, Phys. Rev. C **36**, 1916 (1987).
[4] M. T. Peña, H. Garcilazo, U. Oelfke, and P. U. Sauer, Phys. Rev. C **45**, 1487 (1992).
[5] J. M. Laget, Nucl. Phys. **A446**, 489c (1985).
[6] P. E. Argan, G. Audit, A. Bloch, J. L. Faure, J. M. Laget, J. Martin, G. Tamas, and C. Schuhl, Nucl. Phys. **A296**, 373 (1978).
[7] C. E. Thorn, G. Giordano, O. C. Kistner, G. Matone, A. M. Sandorfi, C. Schaerf, and C. S. Whisnant, Nucl. Instrum. Methods **A285**, 477 (1989).
[8] D. Tedeschi *et al.*, Phys. Rev. Lett. **73**, 408 (1994).
[9] R. A. Cecil, B. D. Anderson, and R. Madey, Nucl. Instrum. Methods **161**, 439 (1979).
[10] P. Benz *et al.*, Nucl. Phys. **B65**, 158 (1973).
[11] Richard A. Arndt, Ron L. Workman, Zhujun Li, and L. David Roper, Phys. Rev. C **42**, 1853 (1990).
[12] Richard A. Arndt, SAID database, (γ, π^0) solution SP89, private communication.
[13] J. M. Laget, Nucl. Phys. **A194**, 81 (1972).
[14] William B. Clayton, Ph.D. thesis, Rensselaer Polytechnic Institute, 1993; Brookhaven National Laboratory Internal Report LEGS-93T2, 1993.
[15] J.-L. Faure *et al.*, Nucl. Phys. **A424**, 383 (1984).